Polymer Chemistry

ROYAL SOCIETY OF CHEMISTRY

PAPER

View Article Online
View Journal | View Issue

Check for updates

Cite this: *Polym. Chem.*, 2023, **14**, 720

Stereo-electronic contributions in yttrium-mediated stereoselective ring-opening polymerization of functional *racemic* β-lactones: ROP of 4-alkoxymethylene-β-propiolactones with bulky exocyclic chains†

Rama M. Shakaroun,[a] Ali Dhaini,[a] Romain Ligny,[a] Ali Alaaeddine,[b] Sophie M. Guillaume *[a] and Jean-François Carpentier *[a]

Stereoselective ring-opening polymerization (ROP) of cyclic esters is the privileged strategy to access stereoregular polyesters that are widely applied in various domains, such as in particular the biomedical and packaging fields. The production of synthetic stereo-enriched polyhydroxyalkanoates (PHAs) derived from *racemic* β-lactones by ROP is still a challenge. In this context, linear, high molar mass, narrowly dispersed PHAs, namely PBPL^{CH_2OiPr}, PBPL^{CH_2OtBu} and PBPL^{CH_2OTBDMS} ($M_{n,SEC}$ up to 94 300 g mol^{-1}; $Đ_M$ = 1.06–1.18; TBDMS = Si*t*BuMe$_2$), with syndiotactic enrichment (P_r = 0.76–0.87) were successfully synthesized by stereoselective ROP of the corresponding functional *racemic* β-propiolactones, *rac*-BPL^{CH_2OiPr}, *rac*-BPL^{CH_2OtBu} and *rac*-BPL^{CH_2OTBDMS}, respectively, which are promoted by diverse achiral diamino-bis(phenolate) yttrium complexes featuring various R′/R″ substituents (Y{ONNO$^{R',R''}$}, **2a–d**). The influence of the steric hindrance of the BPL^{FG} side-functionality, with FG = CH$_2$O*i*Pr, CH$_2$O*t*Bu, and CH$_2$OTBDMS, on the ROP kinetics, stereoselectivity and thermal properties of the resulting PHAs, as a function of **2a–d** catalysts, was compared to that of the previously reported similar but less hindered BPL^{FG} monomers, with FG = CH$_2$OMe, CH$_2$OAllyl, CH$_2$OBn, and CH$_2$OPh. Overall, this study evidenced that, for the newly prepared *rac*-BPL^{CH_2OiPr}, *rac*-BPL^{CH_2OtBu} and *rac*-BPL^{CH_2OTBDMS} monomers, due to steric constraints induced by the monomer alkoxy/silyloxy side-functionality, all ROPs afforded syndio-enriched polyesters, regardless of the catalyst used. Conversely, only combinations of a BPL^{FG} monomer containing two sets of methylene hydrogens within the side-functionality, *i.e.* with FG = *CH$_2$OCH$_2$*X with X = H, CH = CH$_2$ and C$_6$H$_5$ as in BPL^{CH_2OMe}, BPL^{CH_2OAllyl}, and BPL^{CH_2OBn}, with a yttrium catalyst bearing *ortho*/*para*-chloro substituents (**2a**), gave isotactic functional PHAs. With the latter three monomers, a catalyst with highly sterically crowded substituents on the ligand platform (**2a,b**) was necessary to recover syndio-enriched PBPL^{CH_2OMe,OAll,OBn}.

Received 17th December 2022,
Accepted 6th January 2023

DOI: 10.1039/d2py01573k

rsc.li/polymers

Introduction

Stereoselective ring-opening polymerization (ROP) of chiral *racemic* lactones is a field of topical interest as it allows accessing polymers with variable microstructures (*i.e.*, tacticities), and hence polymer materials with differentiated and controlled properties.[1] One of the most ubiquitous examples in this area is probably the ROP of *racemic* lactide (*rac*-LA) which has opened large avenues, in particular toward the formation of isotactic PLA stereocomplexes with significantly enhanced thermal characteristics.[1a–e] The formation of isotactic polyesters from the ROP of *racemic* lactones is clearly much less common than that of their syndiotactic (heterotactic) counterparts; indeed, the latter syndio/hetero tacticities are often the result of a chain-end stereocontrol[1a,b] where the minimization of steric tilting in the transition state induces the regular, alternated enchainment of consecutive monomer units with the opposite configuration. On the other hand, the formation of isotactic polyesters from *racemic* cyclic esters usually requires

[a]*Univ. Rennes, CNRS, Institut des Sciences Chimiques de Rennes, UMR 6226, F-35042 Rennes, France. E-mail: sophie.guillaume@univ-rennes.fr, jean-francois.carpentier@univ-rennes.fr*
[b]*Univ. Libanaise, Campus Universitaire Rafic Hariri Hadath, Faculté des Sciences, Laboratoire de Chimie Médicinale et des Produits Naturels, Beirut, Lebanon*

†Electronic supplementary information (ESI) available: General conditions, synthesis and characterization of BPL^{CH_2OR} monomers, NMR and mass spectra, and DSC traces. See DOI: https://doi.org/10.1039/d2py01573k

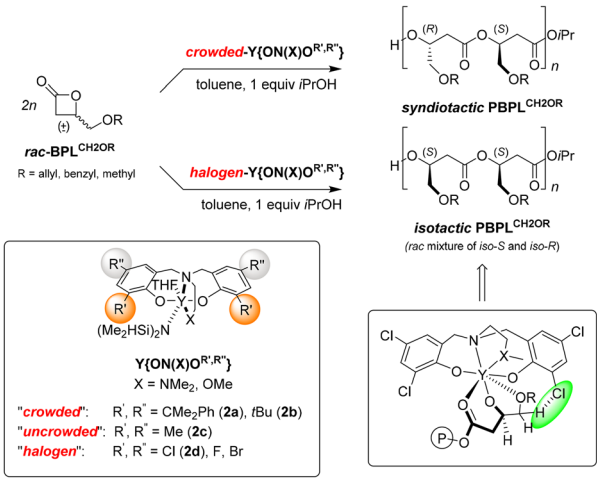

Scheme 1 Previously reported stereoselective ROP of 4-alkoxymethylene-β-propiolactones by Y{ON(X)O$^{R',R''}$} catalytic systems, with stereoselectivity outcomes depending on the stereo-electronic characteristics of the catalyst. The bottom-right structure depicts the transition state with attractive non-covalent Cl···H interactions allegedly driving the isoselectivity.[7]

the use of *chiral* catalysts, most often metal-based ones,[2] to proceed *via* a so-called enantiomorphic site control; isoselective ROP of *racemic* lactones with achiral catalysts is even less frequent and largely focused on *rac*-LA.[1,3] A recent, remarkable addition is the stereoselective ROP of eight-membered *racemic* cyclic diolides mediated by discrete rare earth-based catalysts developed by the group of Chen, which affords a variety of perfectly isotactic (P_m up to 0.99)‡ polyhydroxyalkanoates (PHAs).[4] In our longstanding research on the stereoselective ROP of *racemic* β-lactones[5] with achiral alkoxyamino- or diamino-bisphenolate-yttrium catalysts ({Y{ON(X)O$^{R',R''}$}),[6] we have reported that only the use of catalysts bearing halogeno *ortho*/*para*-substituents (R′,R″ = Cl, F or Br) on the phenolate ligand platform allowed the highly isoselective ROP of the specific *racemic* 4-alkoxymethylene-β-propiolactones (*rac*-BPL^{CH_2OR}, Scheme 1);[7] actually, this was proved to be effective (*i.e.*, isoselective) only for R = 4-methoxy (OMe), -allyloxy (OAll) or benzyloxy (OBn) derivatives, that is, the monomers having two methylene groups apart from the oxygen in the side-functionality (*i.e.*, with a CH_2(referred to as "inner")-O–CH_2(referred to as "outer")X group).[8] As supported by DFT computations, such isoselectivity apparently relies on attractive non-covalent interactions (NCIs)[9] between the halogen *ortho*-substituents on the yttrium ligand with the "inner" and/or "outer" methylene hydrogens within the side-functional group of the last inserted monomer unit within the growing polymer chain (Scheme 1).[7] As a matter of fact, the ROP of *rac*-BPL^{CH_2OR} monomers without such an "outer" methylene group, *e.g.* with R = OPh, or with two

‡P_m is the probability of meso linkages, that is, the enchainment of two monomer units with the same configuration. $P_m = 1 - P_r$, where P_r is the probability of racemo linkage, that is, the enchainment of two monomer units with the opposite configuration.

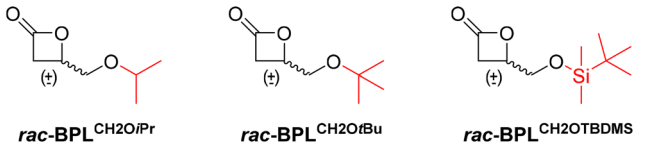

Scheme 2 4-Alkoxymethylene-β-propiolactones with bulky alkoxy side-functionalities depleted of an "outer" methylene group, investigated in the present study.

"inner" methylene groups, *i.e.* *rac*-BPL^{CH_2CH_2OCH_2Ph}, with an isoselective Y{ONNO^{Cl,Cl}} catalytic system, all recovered syndio-enriched polymers (P_r = 0.75–0.77).[10;§] The contribution of the "outer" methylene group in the pendant arm of BPL^{CH_2OCH_2X} is thus still an open question.

To gain a better insight into the factors that govern the isoselectivity observed in the ROP of some *rac*-BPL^{CH_2OR} monomers mediated by the Y{ONNO^{Cl,Cl}} catalytic system and to probe further the possible decisive influence of "outer" methylene hydrogens (–CH_2OCH_2X), we have herein explored the yttrium-mediated ROP of three β-propiolactones which do not feature an "outer" methylene group within the alkoxide moiety and which display an alkoxy tertiary or quaternary carbon/silicon, namely *rac*-BPL^{CH_2OiPr}, *rac*-BPL^{CH_2OtBu}, and *rac*-BPL^{CH_2OTBDMS} (TBDMS = Si*t*BuMe$_2$; Scheme 2),[11] respectively, in comparison with the related *rac*-BPL^{CH_2OPh} which is depleted of the outer methylene (-OCH_2X) moiety.[10] These three *rac*-BPL$^{CH_2OiPr/OtBu/OTBDMS}$ monomers, two of which are new and all of which are readily prepared by carbonylation of the parent glycidyl ethers (see the ESI†),[11,12] have been chosen so as to replace the "outer" methylene hydrogens (as in R = OCH_2H, OCH_2CH = CH_2 and OCH_2Ph) with one or two methyl groups (as in R = O*i*Pr and O*t*Bu). This should allow one to assess whether the "outer" alkoxide methylene may contribute to the iso-stereocontrol of the ROP of such functional BPL^{CH_2OR}s. In addition, *rac*-BPL^{CH_2OTBDMS} was selected to probe, besides the impact of a missing "outer" methylene in the side function of the monomer, the impact of the steric bulkiness on the alkoxy functionality (O*i*Pr and O*t*Bu *vs.* OSiMe$_2$*t*Bu). Further comparison with the β-propiolactone featuring a somewhat bulky aryloxy moiety, namely BPL^{CH_2OPh}, which was shown to give a syndiotactic polyester,[10] could then be made. In addition, PHAs derived from *rac*-BPL^{CH_2OTBDMS} are of further interest as they could subsequently provide access to hydrophilic polyesters upon deprotection of –OTBDMS into pendant hydroxyl groups also available for post-polymerization modification, as for instance to chemically bound a biological moiety for theranostic outcomes. Four catalysts {Y{ONNO$^{R',R''}$}, **2a–d**, having different R′,R″ *ortho*/*para*-substituents installed on the bisphenolate platform and which have previously revealed quite distinctive and effective stereocontrol abilities in the ROP of *racemic* functional β-lactones due to their

§Note that, similarly, the ROP of the parent sulfur BPL^{CH_2SPh} recovered the corresponding syndiotactic PHA; see ref. 10.

different stereo-electronic characteristics,[6,7] have been selected for the present study.

Experimental section

See the ESI† for additional details.

Synthesis and characterization of BPL^{CH_2OR} monomers

BPL^{CH_2OR} monomers were synthesized by carbonylation of the corresponding *racemic* or enantiopure glycidyl ethers (*rac*-/(*S*)-Glyc^{CH_2OR}) using a previously reported procedure.[11,12] All *rac*-BPL^{CH_2OR} and (*S*)-BPL^{CH_2OR} monomers were characterized (refer to the ESI) and stored under argon at −27 °C.

Typical BPL^{CH_2OR} polymerization procedure

In a typical experiment,[13] in a glovebox, a Schlenk flask was charged with $[Y(N(SiHMe_2)_2)_3](THF)_2$ (8.8 mg, 14 μmol) and {ONNO$^{t\mathrm{Bu2}}$} (**1d**, 7.4 mg, 14 μmol), and toluene (0.25 mL) was next added. To this solution, iPrOH (107 μL of a 1% (*v*/*v*) solution in toluene, 1 equiv. *vs.* Y) was added under stirring at room temperature (*ca*. 20 °C). After 5 min of stirring, a solution of *rac*-BPL^{CH_2OR} (0.84 mmol, 60 equiv.) in toluene (0.5 mL) was added rapidly and the mixture was stirred at 20 °C for 1 h. The reaction was quenched by the addition of acetic acid (*ca.* 0.5 mL of a 1.6 mol L^{-1} solution in toluene). The resulting mixture was concentrated to dryness under vacuum and the conversion was determined by ^{1}H NMR analysis of the residue in $CDCl_3$. The crude polymer was then dissolved in CH_2Cl_2 (*ca.* 1 mL), precipitated in cold pentane (*ca.* 5 mL), filtered and dried. PBPL^{CH_2OiPr}, PBPL^{CH_2OtBu} and PBPL^{CH_2OTBDMS} were recovered as a colorless oil, yellowish oil, and colorless solid, respectively. All recovered polymers were then analyzed by NMR spectroscopy, mass spectrometry, SEC, and DSC analyses.

Results and discussion

ROP of *rac*-BPL^{CH_2OiPr}

The ROP of *rac*-BPL^{CH_2OiPr} was explored under the same general operating conditions as those used for the above-mentioned reference ROPs mediated by similar Y{ONNO$^{R',R''}$} catalytic systems, that is, in toluene solution at room temperature, using *in situ* combinations of **2a–d**/*i*PrOH (1 : 1) (Table 1).[10] The reactivity trend observed for the different yttrium catalytic systems followed the one established with other similar β-lactones:[6b,7] the Cl substituted catalyst **2d** was the least active, with only partial conversion of 30 monomer equiv. even after prolonged reaction time (TOF_{2d} = *ca*. 0.2 h^{-1}, entry 1); the Me-substituted catalyst **2c** achieved nearly complete consumption of *ca.* 60 and 100 monomer units within 12 and 24 h, respectively (TOF_{2c} = *ca.* 5 h^{-1}, entry 2); a much higher reactivity was observed with the catalytic systems bearing bulky substituted ligands (cumyl, *t*Bu, **2a–b**), and almost quantitative

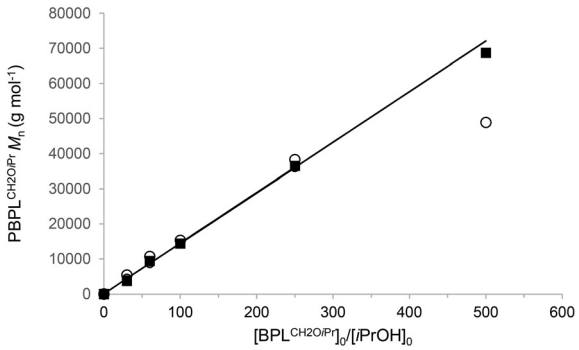

Fig. 1 Illustration of the variation of $M_{n,NMR}$ ■, $M_{n,SEC}$ ○, and $M_{n,theo}$ (the solid line) molar mass values of PBPL^{CH_2OiPr} synthesized from the ROP of *rac*-BPL^{CH_2OiPr} mediated by the **2b**/*i*PrOH (1 : 1) catalytic system as a function of the BPL^{CH_2OiPr} monomer loading/conversion (Table 1, entries 4–8).

Table 1 ROP of *rac*-BPL^{CH_2OiPr} mediated by the **2a–d**/*i*PrOH catalytic systems[a]

Entry	Cat.	$[BPL^{CH_2OiPr}]_0/[\mathbf{2}]_0/[i\mathrm{PrOH}]_0$	Time[b] (min)	BPL^{CH_2OiPr} Conv.[c] (%)	$M_{n,theo}$[d] (g mol^{-1})	$M_{n,NMR}$[e] (g mol^{-1})	$M_{n,SEC}$[f] (g mol^{-1})	$Đ_M$[f]	P_r[g]
1	**2d**	30 : 1 : 1	24 × 60	19	850	1100	1400	1.15	0.70
2	**2c**	60 : 1 : 1	12 × 60	96	8350	7550	9500	1.09	0.71
3	**2c**	100 : 1 : 1	24 × 60	90	13 000	15 000	15 900	1.18	0.72
4	**2b**	30 : 1 : 1	5	100	4400	3700	5400	1.09	0.84
5	**2b**	60 : 1 : 1	5	100	8700	9400	10 700	1.11	0.84
6	**2b**	100 : 1 : 1	15	100	14 450	14 400	15 300	1.13	0.85
7	**2b**	250 : 1 : 1	20	100	36 050	36 500	38 300	1.08	0.85
8	**2b**	500 : 1 : 1	210	100	72 100	68 700	48 900	1.06	0.86
9	**2a**	60 : 1 : 1	5	100	8700	9000	10 050	1.10	0.82
10	**2a**	100 : 1 : 1	15	100	14 450	17 000	18 600	1.13	0.82
11[h]	**2b**	30 : 1 : 1	60	94	4100	4600	5600	1.10	<0.05

[a] Reactions performed with $[BPL^{CH_2OiPr}]_0$ = 1.0 M in toluene at room temperature. [b] Reaction times were not necessarily optimized. [c] Conversion of BPL^{CH_2OiPr} as determined by ^{1}H NMR analysis of the crude reaction mixture. [d] Molar mass calculated according to $M_{n,theo} = ([BPL^{CH_2OiPr}]_0/[\mathbf{2}]_0 \times \mathrm{conv.}_{BPL(CH_2OiPr)} \times M_{BPL(CH_2OiPr)}) + M_{i\mathrm{PrOH}}$ with $M_{BPL(CH_2OiPr)}$ = 144 g mol^{-1} and $M_{i\mathrm{PrOH}}$ = 60 g mol^{-1}. [e] Molar mass determined by ^{1}H NMR analysis of the isolated polymer, from the resonances of the terminal O*i*Pr group. [f] Number-average molar mass (uncorrected values) and dispersity (M_w/M_n) determined by SEC analysis in THF at 30 °C *vs.* polystyrene standards. [g] P_r is the probability of racemic linkages between BPL^{CH_2OiPr} units as determined by $^{13}C\{^1H\}$ NMR analysis of the isolated PBPL^{CH_2OiPr}s. [h] ROP of enantiopure (*S*)-BPL^{CH_2OiPr}.

conversion of 30–250 equiv. of *rac*-BPL^{CH_2OiPr} was typically achieved within 5–20 min (TOF_{2a-b} > 750 h^{-1}, entries 4–10).

The ROP of *rac*-BPL^{CH_2OiPr} with the **2a–d**/*i*PrOH systems proceeded with quite good control in terms of macromolecular parameters. All the polymers showed a linear topology with α-isopropoxycarbonyl and ω-hydroxy chain-end groups, as unambiguously established by ^{1}H and J-MOD NMR spectroscopy and MALDI-ToF mass spectrometry analyses (see the ESI; Fig. S1–S6†). Also, alongside narrow dispersities ($Đ_M$ = 1.06–1.18), the calculated ($M_{n,theo}$) and experimental ($M_{n,NMR}$, $M_{n,SEC}$) molar mass values were in quite good agreement. A linear relationship between the experimental molar mass values and the *rac*-BPL^{CH_2OiPr} monomer loading/conversion up to 250 equiv. was observed with the **2b**/*i*PrOH (1 : 1) catalytic system (Fig. 1). Altogether, these results confirm the limited extent or the absence of irreversible transfer/side-reactions (typical inter- and intra-molecular undesirable transesterification reactions, *i.e.* reshuffling and backbiting reactions, respectively) and suggest essentially active polymerization features.

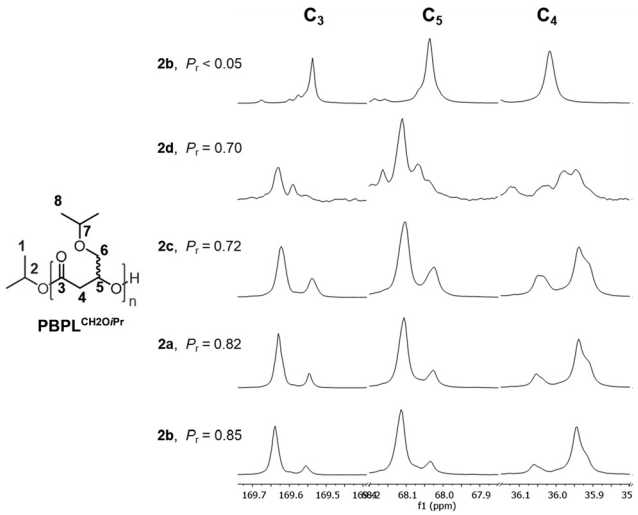

Fig. 2 Zoomed regions of the $^{13}C\{^1H\}$ NMR spectra (125 MHz, $CDCl_3$, 23 °C) of PBPL^{CH_2OiPr} prepared by ROP of *rac*-BPL^{CH_2OiPr}, except for the top spectrum of enantiopure (*S*)-BPL^{CH_2OiPr} (Table 1, entry 11), mediated by the **2a**, **2b**, **2c**, or **2d**/*i*PrOH (1 : 1) catalytic systems (Table 1, entries 9, 7, 3 and 1, respectively).

A close examination of the carbonyl (δ *r* = *ca.* 169.65, δ *m* = *ca.* 169.55 ppm), methine (δ *r* = *ca.* 68.12, δ *m* = *ca.* 68.03 ppm) and methylene (δ *r* = *ca.* 35.94, δ *m* = *ca.* 36.05 ppm) main-chain carbons' signals in the ^{13}C NMR spectra allowed establishing the polymers' tacticity (Fig. 2). For the sake of comparison, a pure isotactic PBPL^{CH_2OiPr} system was prepared from the ROP of enantiopure (*S*)-BPL^{CH_2OiPr} (Table 1, entry 11). Regardless of the catalyst used in the **2a–d** series, the ROP of *rac*-BPL^{CH_2OiPr} gave syndio-enriched polymers. It is noteworthy that the **2c** system (Me substituents) exhibited approximately the same syndiotacticity (P_r = 0.71–0.72) as the one obtained from **2d** (Cl substituents, P_r = 0.69–0.70). This suggests the absence of any electronic effect from **2d** but, instead, the preponderance of a pure, yet limited steric control, in tuning the tacticity of PBPL^{CH_2OiPr}. Along the same line, catalytic systems **2a–b** that bear bulkier cumyl and *tert*-butyl substituents resulted in better syndio-enrichments (P_r = 0.82–0.85), which are close to those obtained for PBPL^{CH_2OMe}, PBPL^{CH_2OAll} and PBPL^{CH_2OBn} (P_r = 0.78–0.90).[7]

ROP of *rac*-BPL^{CH_2OtBu}

The stereoselective ROP of *rac*-BPL^{CH_2OtBu} was similarly examined (Table 2). The activity trend of catalysts **2a–d** (*ca.* 75 monomer equiv.) was very comparable to the aforementioned ROP of *rac*-BPL^{CH_2OiPr}: TOF_{2d} = *ca.* 0.7 h^{-1} (entry 1) *vs.* TOF_{2c} = *ca.* 10 h^{-1} (entry 4) *vs.* TOF_{2a-b} > 900 h^{-1} (entries 6 and

Table 2 ROP of *rac*-BPL^{CH_2OtBu} mediated by the **2a–d**/*i*PrOH catalytic systems[a]

Entry	Cat.	$[BPL^{CH_2OtBu}]_0/[2]_0/[iPrOH]_0$	Time[b] (min)	BPL^{CH_2OtBu} Conv.[c] (%)	$M_{n,theo}$[d] (g mol^{-1})	$M_{n,NMR}$[e] (g mol^{-1})	$M_{n,SEC}$[f] (g mol^{-1})	$Đ_M$[f]	P_r[g]
1	**2d**	25 : 1 : 1	24 × 60	67	2600	2500	2400	1.12	0.70
2	**2d**	75 : 1 : 1	27 × 60	28	3300	3400	3000	1.06	0.71
3	**2c**	25 : 1 : 1	60	100	3600	3100	3200	1.09	0.74
4	**2c**	75 : 1 : 1	7 h	90	10 700	10 900	13 600	1.16	0.75
5	**2b**	30 : 1 : 1	30	100	4300	3900	4300	1.12	0.83
6	**2b**	73 : 1 : 1	5	100	11 600	11 300	14 800	1.10	0.84
7	**2b**	120 : 1 : 1	10	100	18 800	18 800	24 000	1.14	0.83
8	**2b**	250 : 1 : 1	15	99	39 100	40 000	49 900	1.15	0.84
9	**2b**	500 : 1 : 1	15	99	78 300	80 000	94 300	1.18	0.84
10	**2a**	30 : 1 : 1	30	100	4300	4300	4000	1.12	0.78
11	**2a**	75 : 1 : 1	5	100	11 900	10 900	15 200	1.14	0.78
12[h]	**2b**	70 : 1 : 1	30	100	11 100	10 300	14 300	1.09	<0.05

[a] Reactions performed with $[BPL^{CH_2OtBu}]_0$ = 1.0 M in toluene at room temperature. [b] Reaction times were not necessarily optimized. [c] Conversion of BPL^{CH_2OtBu} as determined by ^{1}H NMR analysis of the crude reaction mixture. [d] Molar mass calculated according to $M_{n,theo}$ = ($[BPL^{CH_2OtBu}]_0/[2]_0$ × $conv._{BPL(CH_2OtBu)}$ × $M_{BPL(CH_2OtBu)}$) + M_{iPrOH} with $M_{BPL(CH_2OtBu)}$ = 158 g mol^{-1}and M_{iPrOH} = 60 g mol^{-1}. [e] Molar mass determined by ^{1}H NMR analysis of the isolated polymer, from the resonances of the terminal O*i*Pr group. [f] Number-average molar mass (uncorrected values) and dispersity (M_w/M_n) determined by SEC analysis in THF at 30 °C *vs.* polystyrene standards. [g] P_r is the probability of racemic linkages between BPL^{CH_2OtBu} units as determined by $^{13}C\{^1H\}$ NMR analysis of the isolated PBPL^{CH_2OtBu}s. [h] ROP of enantiopure (*S*)-BPL^{CH_2OtBu}.

11). Also, the corresponding characteristic data of PBPL^{CH_2OtBu} (NMR spectra, M_n and dispersity values, and linear molar mass increase correspondingly to larger monomer loadings) revealed well-defined α-isopropoxycarbonyl, ω-hydroxy telechelic PHAs with chain-end fidelity and an overall quite good control of the polymerization (see the ESI, Fig. S7–S11†).

The stereochemistry of PBPL^{CH_2OtBu} prepared by ROP of *rac*-BPL^{CH_2OtBu} mediated by the **2a–d**/*i*PrOH systems closely resembles that of PBPL^{CH_2OiPr}. All the isolated PBPL^{CH_2OtBu} samples revealed a syndio-enrichment regardless of the catalyst used (**2a–d**) (Fig. 3) (δ *r*(C=O) = *ca.* 169.77, δ *m*(C=O) = *ca.* 169.70 ppm; δ *r*(CH) = *ca.* 62.18, δ *m*(CH) = *ca.* 62.11 ppm; δ *r*(CH_2) = *ca.* 35.97, δ *m*(CH_2) = *ca.* 36.06 ppm). While **2d** (Cl substituents) afforded almost the same enrichment of PBPL^{CH_2OtBu} as that of PBPL^{CH_2OiPr} (P_r = *ca.* 0.70), catalyst **2c** (Me substituents) contributed to a slightly higher syndiotacticity (P_r = 0.75 *vs.* 0.71), while catalyst **2a** (cumyl substituents) exhibited a slightly inferior syndio-regularity (P_r = 0.78 *vs.* 0.82). Finally, catalyst **2b** (*t*Bu substituents) produced the highest enrichment of PBPL^{CH_2OtBu} (P_r = 0.84), again reminiscent of that of PBPL^{CH_2OiPr} (P_r = 0.85). Hence, the general reactivity trend of the **2a–d** catalysts to yield syndio-enriched PBPL^{CH_2OtBu} is the same as the one observed for PBPL^{CH_2OiPr}, but with minor differences in the PHA enrichment in the case of catalysts **2a,c**.

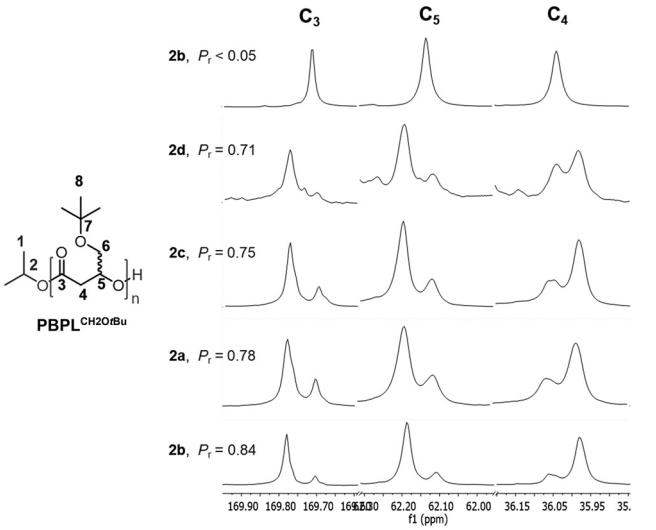

Fig. 3 Zoomed regions of the $^{13}C\{^1H\}$ NMR spectra (125 MHz, $CDCl_3$, 23 °C) of PBPL^{CH_2OtBu} prepared by ROP of *rac*-BPL^{CH_2OtBu}, except for the top spectrum of enantiopure (*S*)-BPL^{CH_2OtBu} (Table 2, entry 12), mediated by the **2a**, **2b**, **2c**, or **2d**/*i*PrOH (1 : 1) catalytic systems (Table 2, entries 2, 4, 6 and 11, respectively).

ROP of *rac*-BPL^{CH_2OTBDMS}

Representative results of the investigation of the ROP of *rac*-BPL^{CH_2OTBDMS} mediated by the **2a–d**/*i*PrOH catalytic systems are summarized in Table 3. With both **2c–d** systems (Me, Cl substituents), incomplete low monomer conversions were obtained for *rac*-BPL^{CH_2OTBDMS} loadings of 30–60 equiv. after 2–3 days (entries 1–3), exhibiting very low TOF_{2c-d} of *ca.* 0.1–0.2 h^{-1}. The **2a–b** systems (*t*Bu and cumyl substituents) led to complete or almost complete conversions of 30–500 equiv. of *rac*-BPL^{CH_2OTBDMS} after 1–8 h (entries 4–9), with higher TOF_{2a-b} > 100 h^{-1}. Hence, the **2a–d**/*i*PrOH catalytic systems featured a regular trend toward the ROP of *rac*-BPL^{CH_2OTBDMS}, yet with an overall lower activity as compared to the ROP of *rac*-BPL^{CH_2OiPr} and *rac*-BPL^{CH_2OtBu}.

The M_n and dispersity data summarized in Table 3, the linear variation of the $M_{n,NMR}$ and $M_{n,SEC}$ molar mass values of PBPL^{CH_2OTBDMS} as a function of the monomer loading/conversion and the NMR spectra (see the ESI Fig. S12–S16†), all testify a similar well-controlled polymerization of *rac*-BPL^{CH_2OTBDMS} to the **2a–d**/*i*PrOH catalytic systems, as that observed for *rac*-BPL^{CH_2OiPr} and *rac*-BPL^{CH_2OtBu}, affording well-defined α-isopropoxycarbonyl, ω-hydroxy end-capped PHAs. Also, similar to PBPL^{CH_2OiPr} and PBPL^{CH_2OtBu} discussed above,

Table 3 ROP of *rac*-BPL^{CH_2OTBDMS} mediated by the **2a–d**/*i*PrOH catalytic systems[a]

Entry	Cat.	$[BPL^{CH_2OTBDMS}]_0/[\mathbf{2}]_0/[i\text{PrOH}]_0$	Time[b] (h)	BPL^{CH_2OTBDMS} Conv.[c] (%)	$M_{n,theo}$[d] (g mol^{-1})	$M_{n,NMR}$[e] (g mol^{-1})	$M_{n,SEC}$[f] (g mol^{-1})	$Đ_M$[f]	P_{rM}[g]
1	**2d**	30 : 1 : 1	48	16	1800	2500	1000	1.07	0.76
2	**2c**	30 : 1 : 1	8	30	2000	1600	2500	1.14	n.d.[i]
3	**2c**	60 : 1 : 1	72	25	3300	3750	3000	1.12	0.77
4	**2b**	60 : 1 : 1	4	96	12 500	13 500	9000	1.13	0.83
5	**2b**	120 : 1 : 1	8	95	24 700	23 400	19 200	1.12	0.84
6	**2b**	250 : 1 : 1	5	100	47 100	37 600	24 300	1.07	0.81
7	**2b**	500 : 1 : 1	5	100	94 300	86 900	30 000	1.06	0.81
8	**2a**	30 : 1 : 1	1	98	6400	7600	8000	1.11	0.87
9	**2a**	60 : 1 : 1	4	99	12 900	12 350	10 000	1.10	0.87
10[h]	**2a**	50 : 1 : 1	4	99	10 300	9100	8400	1.15	<0.05

[a] Reactions performed with $[BPL^{CH_2OTBDMS}]_0$ = 1.0 M in toluene at room temperature. [b] Reaction times were not necessarily optimized. [c] Conversion of BPL^{CH_2OTBDMS} as determined by ^1H NMR analysis of the crude reaction mixture. [d] Molar mass calculated according to $M_{n,theo} = ([BPL^{CH_2OTBDMS}]_0/[\mathbf{2}]_0 \times conv._{BPL(CH_2OTBDMS)} \times M_{BPL(CH_2OTBDMS)}) + M_{i\text{PrOH}}$ with $M_{BPL(CH_2OTBDMS)}$ = 216 g mol^{-1} and $M_{i\text{PrOH}}$ = 60 g mol^{-1}. [e] Molar mass determined by ^1H NMR analysis of the isolated polymer, from the resonances of the terminal O*i*Pr group. [f] Number-average molar mass (uncorrected values) and dispersity (M_w/M_n) determined by SEC analysis in THF at 30 °C *vs.* polystyrene standards. [g] P_r is the probability of racemic linkages between BPL^{CH_2OTBDMS} units as determined by $^{13}C\{^1H\}$ NMR analysis of the isolated PBPL^{CH_2OTBDMS}s. [h] ROP of enantiopure (*S*)-BPL^{CH_2OTBDMS}. [i] Not determined.

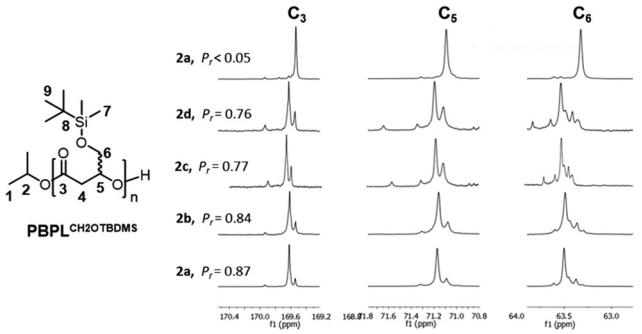

Fig. 4 Zoomed regions of the $^{13}C\{^1H\}$ NMR spectra (125 MHz, $CDCl_3$, 23 °C) of PBPL^{CH_2OTBDMS} prepared by ROP of *rac*-BPL^{CH_2OTBDMS}, except for the top spectrum of enantiopure (*S*)-BPL^{CH_2OTBDMS} (Table 3, entry 10), mediated by the **2a**, **2b**, **2c**, or **2d**/*i*PrOH (1 : 1) catalytic systems (Table 3, entries 9, 5, 3 and 1, respectively); *stands for residual monomer resonances.

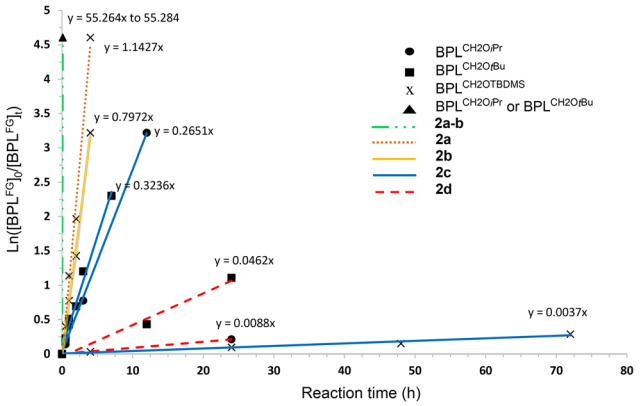

Fig. 5 Semi-logarithmic first-order plots for the ROP of *rac*-BPL^{FG}s (FG = CH_2OiPr, CH_2OtBu, and $CH_2OTBDMS$) mediated by **2a–d**/*i*PrOH (20 °C, toluene; $[BPL^{FG}]_0/\{[\mathbf{2a–c}]_0/[i\text{PrOH}]_0\}$ = 60–75 : 1 : 1 and $[BPL^{FG}]_0/\{[\mathbf{2d}]_0/[i\text{PrOH}]_0\}$ = 25–30 : 1 : 1): **2a** (Table 1, entry 9; Table 2, entry 11; Table 3, entry 9); **2b** (Table 1, entry 6; Table 2, entry 6; Table 3, entry 4); **2c** (Table 1, entry 2; Table 2, entry 4; Table 3, entry 3) and **2d** (Table 1, entry 1; Table 2, entry 1); plots from **2a–b** all overlap due to similar higher activity of these catalysts regardless of the monomer functionality, and are represented as ▲. The slow kinetics of the ROP of *rac*-BPL^{OTBDMS} with **2d** (Table 3, entry 1) is not shown.

all the PBPL^{CH_2OTBDMS} systems revealed to be syndio-enriched (P_r = 0.76–0.87; Fig. 4) (δ *r*(C=O) = *ca.* 169.61, δ *m*(C=O) = *ca.* 169.52 ppm; δ *r*(CH) = *ca.* 71.16, δ *m*(CH) = *ca.* 71.08 ppm; δ *r*(CH_2O) = *ca.* 63.50, δ *m*(CH_2O) = *ca.* 63.35 ppm). Obviously, the stereochemistry of the ROP of *rac*-BPL^{CH_2OTBDMS} is controlled by steric components only, where the ascending catalyst selectivity trend is as follows: **2d** (Cl substituents); P_r = 0.76 < **2c** (Me substituents); P_r = 0.77 < **2b** (*t*Bu substituents); P_r = 0.84 < **2a** (cumyl substituents); P_r = 0.87.

Kinetics of the ROP of *rac*-BPL$^{CH_2OiPr/OtBu/OTBDMS}$

Monitoring of NMR-scale polymerizations of *rac*-BPL$^{CH_2OiPr/OtBu/OTBDMS}$ performed with **2a–d**/*i*PrOH confirmed the kinetic trends assessed from the batch experiments (Tables 1–3). Linear semi-logarithmic plots established that all reactions were first-order in the monomer, with apparent rate constants k_{app} > 55 min^{-1} for BPL$^{CH_2OiPr/OtBu}$/**2a–b** (complete conversion was observed after only 5 min under these conditions; see Table 1, entry 9 and Table 2, entry 11); k_{app} = 1.143 ± 0.072 min^{-1} for BPL^{CH_2OTBDMS}/**2a**; 0.797 ± 0.031 min^{-1} for BPL^{CH_2OTBDMS}/**2b**; 0.323 ± 0.033 min^{-1} for BPL^{CH_2OtBu}/**2c**; 0.265 ± 0.032 min^{-1} for BPL^{CH_2OiPr}/**2c**; 0.046 ± 0.041 min^{-1} for BPL^{CH_2OtBu}/**2d**; 0.0088 ± 0.0021 min^{-1} for BPL^{CH_2OiPr}/**2d**; 0.0037 ± 0.0033 min^{-1} for BPL^{CH_2OTBDMS}/**2c** (Fig. 5). Overall, the major trend for the ability of the monomers to ring-open polymerize was thus BPL^{CH_2OtBu} ≥ BPL^{CH_2OiPr} ≫ BPL^{CH_2OTBDMS}, while the catalysts' activity thus generally followed the order **2a–b** ≫ **2c** ≫ **2d**, as previously observed for the ROP of various BPL^{FG}s β-lactones (FG = CH_2OAll, CH_2OBn, CH_2OMe, CH_2OPh, CH_2CH_2OBn, and CH_2SPh) promoted by these catalytic systems (*vide supra*).[7,10]

The thermal characteristics of PBPL^{CH_2OR}s synthesized by ROP of *rac*-BPL^{CH_2OR} (R = *i*Pr, *t*Bu, and TBDMS) were enhanced by the **2a–d** catalytic systems.

The thermal signature of the new functional PHAs synthesized in this work was briefly investigated by differential scanning calorimetry (DSC, Fig. S17–S20†). The glass transition temperature (T_g) values of syndio-enriched

Table 4 Overall sketch of the stereoselective ROP of *rac*-BPL$^{CH_2OMe/CH_2OAll/CH_2OBn/CH_2OiPr/CH_2OtBu/CH_2OTBDMS}$ as a function of catalytic systems {Y{ON(X)O$^{R',R''}$} **2a–d**, with P_r, T_g and T_m values of the resulting PBPL$^{CH_2OMe/CH_2OAll/CH_2OBn/CH_2OiPr/CH_2OtBu/CH_2OTBDMS}$

rac-BPL^{FG}s Cat **2** (R′ = R″)	*rac*-BPL^{CH_2OMe} [7]	*rac*-BPL^{CH_2OAll} [7]	*rac*-BPL^{CH_2OBn} [7]	*rac*-BPL^{CH_2OiPr} (this work)	*rac*-BPL^{CH_2OtBu} (this work)	*rac*-BPL^{CH_2OTBDMS} (this work)
Crowded (cumyl, *t*Bu) (2a–b)	Syndiotactic P_r = 0.78–0.81 T_g = −12 °C T_m = 116 °C	Syndiotactic P_r = 0.81–0.84 T_g = −38 °C T_m = 85 °C	Syndiotactic P_r = 0.85–0.90 T_g = 0 °C no T_m obsv.	Syndiotactic P_r = 0.82–0.86 T_g = −18 °C[a] no T_m obsv. a	Syndiotactic P_r = 0.78–0.84 T_g = −6 °C[b] no T_m obsv. b	Syndiotactic P_r = 0.81–0.87 T_g = 9 °C[c] T_m = 119 °C c
Aliphatic non-crowded (Me; **2c**)	Atactic P_r = 0.49 T_g = −18 °C	Atactic P_r = 0.49 T_g = −40 °C	Atactic P_r = 0.50 T_g = −6 °C	Syndiotactic P_r = 0.71–0.72 T_g, T_m = n.d.[d]	Syndiotactic P_r = 0.74–0.75 T_g, T_m = n.d.[d]	Syndiotactic P_r = 0.77 T_g, T_m = n.d.[d]
Halogenated non-crowded (Cl, **2d**)	Isotactic P_r = 0.10 T_g = −18 °C	Isotactic P_r = 0.09 T_g = −39 °C	Isotactic P_r = 0.10 T_g = 0 °C	Syndiotactic P_r = 0.70 T_g, T_m = n.d.[d]	Syndiotactic P_r = 0.70–0.71 T_g, T_m = n.d.[d]	Syndiotactic P_r = 0.76 T_g, T_m = n.d.[d]

[a] Table 1, entry 8. [b] Table 2, entry 5. [c] Table 3, entry 6; similar values (T_g = 8 °C, T_m = 118 °C) were recorded for the sample in Table 3, entry 7. [d] Not determined.

PBPL$^{CH_2OiPr/CH_2OtBu/CH_2OTBDMS}$ slightly changed from one to another PHA, and ranged from −18 to +9 °C (Table 4). When compared to the corresponding values gathered for PBPL$^{CH_2OMe/CH_2OAllyl/CH_2OBn}$ (T_g ranging from −38 to 0 °C, Table 4), these values appear to grossly increase with the steric hindrance imparted by the alkoxy/silyloxy side-functionality which decreases the motion of the macromolecules. Also, among the different syndio-enriched polymers herein prepared, only PBPL^{CH_2OTBDMS} featured a semi-crystalline behavior with T_m values of 118–119 °C (Fig. S19 and S20†).

Conclusions

Table 4 summarizes the stereoselectivity outcome of the ROP of *rac*-BPL$^{CH_2OMe/CH_2OAll/CH_2OBn/CH_2OiPr/CH_2OtBu/CH_2OTBDMS}$ as a function of yttrium catalytic systems, differentiating the latter ones according to the presence of highly sterically crowded substituents (*i.e.*, *t*Bu, cumyl; **2a–b**), simple aliphatic non-crowded substituents (Me, **2c**) and halogeno non-crowded substituents (Cl, **2d**). Highly syndio-enriched PBPL$^{CH_2OiPr/OtBu/OTBDMS}$ were obtained from **2a–b**, alike PBPL$^{CH_2OMe/OAll/OBn}$ (P_r = 0.78–0.87 *vs.* 0.78–0.90; respectively). However, substitution of one or two hydrogen atoms in the alkoxide "outer" methylene group of *rac*-BPL$^{CH_2OMe/OAll/OBn}$ by one or two methyl groups – as in *rac*-BPL^{CH_2OiPr} and *rac*-BPL^{CH_2OtBu} – or with *rac*-BPL^{CH_2OTBDMS} resulted in: (i) changing the stereoregularity of the polymer from atactic to syndio-enriched polymers with catalyst **2c** (P_r = 0.49/0.50 *vs.* 0.71–0.77, respectively), and (ii) switching from isotactic to syndio-enriched polymers with catalyst **2d** (P_r = 0.09–0.10 *vs.* 0.76–0.71, respectively). Obviously, these observations evidence that the stereocontrol in the ROP of *racemic* 4-alkoxymethylene-β-propiolactones is driven, systematically by steric considerations, but in a few specific cases by electronic ones as well. For *rac*-BPL^{CH_2OiPr}, *rac*-BPL^{CH_2OtBu} and *rac*-BPL^{CH_2OTBDMS}, apparently due to the large steric constraints induced by the alkoxy(silyloxy) side-functionality, all reactions lead to the formation of syndio-enriched polymers, regardless of the catalyst – a crowded one or a non-crowded one – used. This is what is expected from a 'regular' chain-end stereocontrol mechanism, in which minimization of steric repulsions in the transition state favors the enchainment of monomer units alternately with opposite absolute configurations (and hence the formation of syndiotactic/heterotactic polymers).[1] Only the specific combination of a BPL^{FG} monomer containing two methylene hydrogens apart from the central oxygen on the methylene alkoxy side-functionality (*i.e.*, FG = CH_2OMe, $CH_2OAllyl$, and CH_2OBn) with a catalyst bearing chloro-substituents (**2a**) produced isotactic PHAs; this is assumed to arise from attractive interactions between the ligand chloro substituents and the hydrogen atoms on the alkoxy (methoxy, allyloxy, and benzyloxy) side chain of the ring-opened monomer/growing polymer chain.[7] On the other hand, a catalyst with highly sterically crowding substituents on the ligand platform is necessary to recover syndio-enriched PHAs from the latter BPL^{CH_2OMe,CH_2OAll,CH_2OBn} monomers, which show no major steric bulkiness on the side chain alkoxymethylene moiety. Thus, at this stage of our investigations, in a ROP mediated by a typically isoselective yttrium catalyst, bulkiness of the –OR methylene-alkoxy/silyloxy moiety of BPL^{CH_2OR} monomers is not sufficient to impart isoselectivity, while the presence of two methylene groups adjacent to the oxygen within these BPL^{CH_2OMe,CH_2OAllyl,CH_2OBn} still appears mandatory to access desirable synthetic isotactic PHAs that mimic their natural analogues. Ongoing work by our group aims at examining further the contribution of the two methylene groups, apart from the oxygen in the side-functionality, in the stereoselective ROP of functional β-lactones towards the synthesis of isotactic functional PHAs.

Author contributions

CRediT: Rama M. Shakaroun: investigation (lead) and writing – original draft (supporting); Ali Dhaini: investigation (supporting) and writing – review & editing (supporting); Romain Ligny: investigation (supporting); Ali Alaaeddine: supervision (supporting); Sophie Guillaume: conceptualization (lead), supervision (lead), writing – original draft (supporting), and writing – review & editing (lead); Jean-François Carpentier: conceptualization (lead), supervision (lead), writing – original draft (lead), and writing – review & editing (lead).

Conflicts of interest

There are no conflicts of interest to declare.

Acknowledgements

This research was financially supported in part by the University of Rennes (Ph.D. grants to R. S., A. D. and R. L.), the Lebanese University (Ph.D. grants to R. S. and A. D.) and the Région Bretagne (Ph.D. ARED grant to R. L.). We are grateful to CRMPO and UAR ScanMAT, especially to Philippe Jéhan, Elsa Caytan, and Marielle Blot for MS, NMR and chiral HPLC chromatography analyses, respectively.

References

1 For leading reviews on stereoselective metal-catalyzed ROP of lactones and related derivatives, see: (*a*) O. Dechy-Cabaret, B. Martin-Vaca and D. Bourissou, *Chem. Rev.*, 2004, **104**, 6147–6176; (*b*) P. Dubois, O. Coulembier and J.-M. Raquez, *Handbook of Ring-Opening Polymerization*, Wiley, Weinheim, 2009; (*c*) C. M. Thomas, *Chem. Soc. Rev.*, 2010, **39**, 165–173; (*d*) M. J. Stanford and A. P. Dove, *Chem. Soc. Rev.*, 2010, **39**, 486–494; (*e*) P. J. Dijkstra, H. Du and J. Feijen, *Polym. Chem.*, 2011, **2**, 520–527; (*f*) A. Buchard, C. M. Bakewell, J. Weiner and C. K. Williams, *Top. Organomet. Chem.*, 2012, **39**, 175–224; (*g*) S. M. Guillaume,

E. Kirillov, Y. Sarazin and J.-F. Carpentier, *Chem. – Eur. J.*, 2015, **21**, 7988–8003; (*h*) J. C. Worch, H. Prydderch, S. Jimaja, P. Bexis, M. L. Becker and A. P. Dove, *Nat. Rev. Chem.*, 2019, **3**, 514–535; (*i*) M. J.-L. Tschan, R. M. Gauvin and C. M. Thomas, *Chem. Soc. Rev.*, 2021, **50**, 13587–13608; (*j*) L. Al-Shok, D. M. Haddleton and F. Adams, Progress in Catalytic Ring-Opening Polymerization of Biobased Lactones, in *Advances in Polymer Science*, 2022, Springer; (*k*) A. H. Westlie, E. C. Quinn, C. R. Parker and E. Y.-X. Chen, *Prog. Polym. Sci.*, 2022, **134**, 101608.

2 For recent examples of achiral organocatalysts for highly isoselective ROP of *racemic* lactide, see: (*a*) B. Koca, D. Akgul and V. Aviyente, *Eur. Polym. J.*, 2019, **121**, 109291 and references cited therein; (*b*) Y. Liu, J. Zhang, X. Kou, S. Liu and Z. Li, *ACS Macro Lett.*, 2022, **11**, 1183–1189; (*c*) F. Ren, X. Li, J. Xian, X. Han, L. Cao, X. Pan and J. Wu, *J. Polym. Sci.*, 2022, **60**, 2847–2854.

3 For selected examples of metal-based catalysts bearing non-chiral ligands for isoselective ROP of *rac*-LA, see: (*a*) N. Nomura, R. Ishii, Y. Yamamoto and T. Kondo, *Chem. – Eur. J.*, 2007, **13**, 4433–4451; (*b*) P. McKeown, M. G. Davidson, G. Kociok-Köhn and M. D. Jones, *Chem. Commun.*, 2016, **52**, 10431–10434; (*c*) D. Myers, A. J. P. White, C. M. Forsyth, M. Bown and C. K. Williams, *Angew. Chem., Int. Ed.*, 2017, **56**, 5277–5282; (*d*) Z. Mou, B. Liu, M. Wang, H. Xie, P. Li, L. Li, S. Lia and D. Cui, *Chem. Commun.*, 2014, **50**, 11411–11414; (*e*) Z. Zhuo, C. Zhang, Y. Luo, Y. Wang, Y. Yao, D. Yuan and D. Cui, *Chem. Commun.*, 2018, **54**, 11998–12001; (*f*) C. Kan, J. Hu, Y. Huang, H. Wang and H. Ma, *Macromolecules*, 2017, **50**, 7911–7919.

4 (*a*) X. Tang and E. Y.-X. Chen, *Nat. Commun.*, 2018, **9**, 2345–2356; (*b*) E. Y.-X. Chen and X. Tang, *US Pat. Appl*, 2019, 0211144; (*c*) X. Tang, A. H. Westlie, E. M. Watson and E. Y.-X. Chen, *Science*, 2019, **366**, 754–758; (*d*) Z. Zhang, C. Shi, M. Scoti, X. Tang and E. Y.-X. Chen, *J. Am. Chem. Soc.*, 2022, **144**, 20016–20024.

5 (*a*) For a review on stereoselective ROP of β-lactones, see: J.-F. Carpentier, *Macromol. Rapid Commun.*, 2010, **31**, 1696–1705. β-Butyrolactone (BL, *aka* BPLMe) is the most common chiral β-lactone; few catalyst systems have shown isoselectivity towards *rac*-BL with P_m values (*i.e.*, the probability of meso/isotactic enchainment) in the range 0.65–0.85; see: (*b*) Z. Zhuo, C. Zhang, Y. Luo, Y. Wang, Y. Yao, D. Yuan and D. Cui, *Chem. Commun.*, 2018, **54**, 11998–12001; (*c*) N. Ajellal, G. Durieux, L. Delevoye, G. Tricot, C. Dujardin, C. M. Thomas and R. M. Gauvin, *Chem. Commun.*, 2010, **46**, 1032–1034; (*d*) M. Zintl, F. Molnar, T. Urban, V. Bernhart, P. Preishuber-Pflügl and B. Rieger, *Angew. Chem., Int. Ed.*, 2008, **47**, 3458–3460, (*Angew. Chem.*, 2008, **120**, 3508–3510); (*e*) R. Reichardt, S. Vagin, R. Reithmeier, A. K. Ott and B. Rieger, *Macromolecules*, 2010, **43**, 9311–9317; (*f*) S. Vagin, M. Winnacker, A. Kronast, P. T. Altenbuchner, P. Deglmann, C. Sinkel, R. Loos and B. Rieger, *ChemCatChem*, 2015, **7**, 3963–3971.

6 (*a*) A. Amgoune, C. M. Thomas, S. Ilinca, T. Roisnel and J.-F. Carpentier, *Angew. Chem., Int. Ed.*, 2006, **45**, 2782–2784; *Angew. Chem.*, 2006, **118**, 2848–2850. For recent accounts, see: (*b*) J.-F. Carpentier, *Organometallics*, 2015, **34**, 4175–4189; (*c*) H. Li, R. M. Shakaroun, S. M. Guillaume and J.-F. Carpentier, *Chem. – Eur. J.*, 2020, **26**, 128–138.

7 (*a*) R. Ligny, M. M. Hänninen, S. M. Guillaume and J.-F. Carpentier, *Angew. Chem., Int. Ed.*, 2017, **56**, 10388–10393, (*Angew. Chem.*, 2017, **129**, 10524–10529); (*b*) R. Ligny, M. M. Hänninen, S. M. Guillaume and J.-F. Carpentier, *Chem. Commun.*, 2018, **54**, 8024–8031.

8 For a recent example of isoselective ROP of *racemic* β-thiobutyrolactone by the same type of achiral alkoxy-amino-bisphenolate-yttrium catalysts, see: H. Li, J. Ollivier, S. M. Guillaume and J.-F. Carpentier, *Angew. Chem., Int. Ed.*, 2022, **61**, e202202386.

9 Other types of NCIs have also been proposed to play a beneficial role in stereoselective ROP of *rac*-LA promoted by Zn-β-diketiminate and Al-bis(cathecolato-amino) catalysts; see: (*a*) E. L. Marshall, V. C. Gibson and H. S. Rzepa, *J. Am. Chem. Soc.*, 2005, **127**, 6048–6051; (*b*) S. Gesslbauer, R. Savela, Y. Chen, A. J. P. White and C. Romain, *ACS Catal.*, 2019, **9**, 7912–7920.

10 R. M. Shakaroun, H. Li, P. Jéhan, M. Blot, A. Alaaeddine, J.-F. Carpentier and S. M. Guillaume, *Polym. Chem.*, 2021, **12**, 4022–4034.

11 *Rac*-BPL^{CH_2OiPr} and *rac*-BPL^{CH_2OtBu} are new monomers. For the synthesis and organocatalyzed ROP of *rac*-BP^{CH_2OTBDMS}, see: R. M. Shakaroun, H. Li, P. Jéhan, A. Alaaeddine, J.-F. Carpentier and S. M. Guillaume, *Polym. Chem.*, 2020, **11**, 2640–2652.

12 (*a*) J. A. Schmidt, E. B. Lobkovsky and G. W. Coates, *J. Am. Chem. Soc.*, 2005, **127**, 11426–11435; (*b*) J. W. Kramer and G. W. Coates, *Tetrahedron*, 2008, **64**, 6973–6978.

13 M. Bouyahyi, N. Ajellal, E. Kirillov, C. M. Thomas and J.-F. Carpentier, *Chem. – Eur. J.*, 2011, **17**, 1872–1883.